PHYSICAL REVIEW C VOLUME 44, NUMBER 2 AUGUST 1991

Light particle correlations for the ^{3}He+Ag reaction at 200 MeV

F. Zhu, W. G. Lynch, T. Murakami, C. K. Gelbke, Y. D. Kim, T. K. Nayak, R. Pelak, M. B. Tsang, H. M. Xu, W. G. Gong, and W. Bauer
Department of Physics and Astronomy and National Superconducting Cyclotron Laboratory, Michigan State University, East Lansing, Michigan 48824

K. Kwiatkowski, R. Płaneta, S. Rose, V. E. Viola, Jr., L. W. Woo, S. Yennello, and J. Zhang
Indiana University Cyclotron Facility, Indiana University, Bloomington, Indiana 47405
(Received 4 June 1991)

Two-proton correlation functions, measured at small relative momenta in the ^{3}He+Ag reaction at 200 MeV, increase monotonically with the kinetic energy of the detected particles. Very strong correlations are observed for intermediate energy protons. These correlations scale with the weaker correlation functions measured for heavier projectiles, and can be reproduced by the Boltzmann-Uehling-Uhlenbeck equation. Even stronger correlations measured for beam velocity protons, however, may be remnants of the initial-state wave functions of the ^{3}He projectiles.

Light particle correlations depend on the size and lifetime of regions emitting light particles during an energetic nuclear reaction [1–15]. Measured correlation functions, for relativistic proton [15] and intermediate energy heavy-ion [4,6–12] induced reactions, increase monotonically with ejectile velocity, consistent with an evolution from more to less energetic emission as the reaction proceeds from initial contact towards an equilibrated target-like residue. Solutions of the Boltzmann-Uehling-Uhlenbeck equation reproduce the energy dependence of proton-proton correlations measured for ^{14}N induced reactions at $E/A=75$ MeV [12]. The calculated correlation functions are sensitive to the in-medium nucleon-nucleon cross section [5,12].

For collisions at nonrelativistic energies, correlation functions gated on the energy of the detected particles reveal that the space-time extent of sources producing the most energetic particles increases with the size of the projectile [10]. The most dramatic sensitivity to the space-time evolution of a nuclear reaction might therefore be expected for light-ion-induced reactions on heavy targets, reflecting the evolution from initial configurations involving the projectile and a few target nucleons to the equilibrated target-like residue. A comparison of two-proton correlation functions for p+Ag and ^{14}N+Ag reactions at 500 MeV, which included all protons above the detection

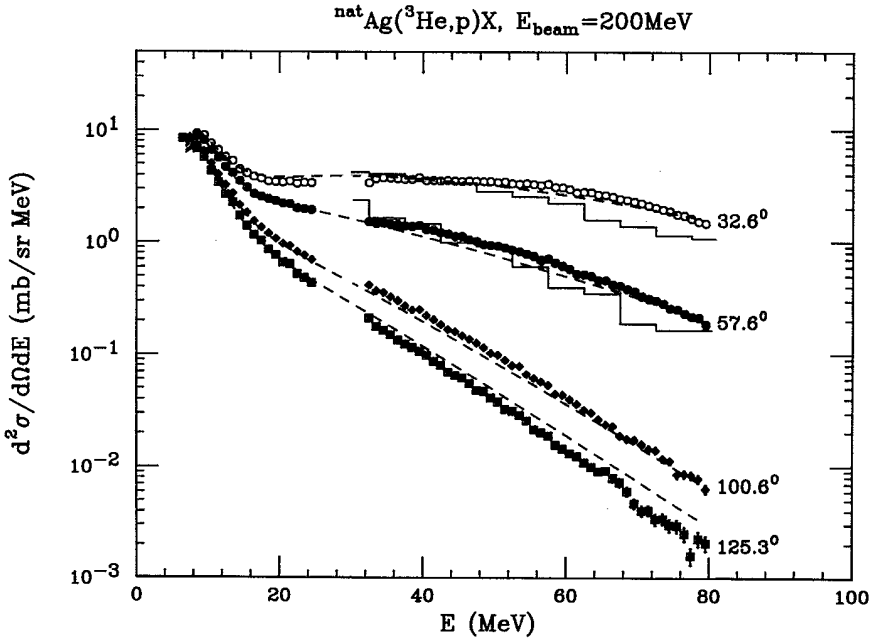

FIG. 1. Single-proton inclusive cross sections for the ^{3}He +Ag reaction at 200 MeV at the indicated laboratory angles. The dashed curves are the corresponding moving source fits using Eq. (1) of Ref. 10 with (N_1,N_2,N_3: 11.93, 0.9137, 1.158 mb/MeV sr), (β_1,β_2,β_3: 0.0080, 0.0408, 0.2450), and (T_1,T_2,T_3: 2.22, 10.42, 13.31 MeV). The histograms denote the energy spectra for nucleons (renormalized by a factor ≈ 0.4) predicted by the BUU simulations.

thresholds, however, displayed little sensitivity to the size of the projectile [14]. In this paper, we investigate two-proton correlations for ^{3}He induced reactions as functions of the energies of the detected protons and compare these measurements to other measurements performed with heavier projectiles. This comparison suggests a natural scaling of the correlation functions for energetic protons with the projectile mass.

The experiment was performed at the Indiana University Cyclotron Facility. A natural 1.05 mg/cm^2 Ag target was bombarded by 200-MeV ^{3}He ions. Coincident light particles were detected with a high-resolution hodoscope consisting of 13 closely packed telescopes [16]. Four of these telescopes were each comprised of four silicon detectors (75 μm, 100 μm, 5 mm, and 5 mm thick). The other nine telescopes were each comprised of two silicon detectors (200 μm and 5 mm thick) and a 10-cm-thick NaI(Tl) detector. Two single-wire gas counters were placed in front of each telescope to provide x and y position information. Energy calibrations of the silicon detectors were obtained using an ^{241}Am source and extended to higher energies with a precision pulser. The NaI(Tl) detectors were calibrated with the ΔE information from the 5-mm Si(Li) detectors and by detecting recoil protons produced in the bombardment of a polypropylene target by 200-MeV ^{3}He ions. Measurements were performed with the hodoscope centered at $\Theta_A = 42°$ and 109° in the laboratory frame.

Measured proton inclusive cross sections are shown in Fig. 1. At low energies, $E < 16$ MeV, the spectra are dominated by evaporation from equilibrated or nearly equilibrated target residues. At higher energies, non-equilibrium emission processes dominate, with some contributions from projectile breakup. These higher-energy contributions become less important with increasing angle.

We define the experimental correlation function $R(q)$ in terms of the measured coincidence yield $Y_{12}(\mathbf{p}_1,\mathbf{p}_2)$ and the singles yield $Y_1(\mathbf{p}_1)$ and $Y_2(\mathbf{p}_2)$:

$$\sum Y_{12}(\mathbf{p}_1,\mathbf{p}_2) = C[1+R(q)]\sum Y_1(\mathbf{p}_1)Y_2(\mathbf{p}_2) . \quad (1)$$

Here, $\mathbf{p}_1$ and $\mathbf{p}_2$ are the momenta of the two particles in the laboratory and q is the relative momentum between the two particles. For each experimental gating condition, the sums on both sides of Eq. (1) are extended over all energy, position, and detector combinations corresponding to specific relative momentum bins. The normalization constant C in Eq. (1) is chosen so that $R(q)$ vanishes at large relative momenta where final-state interactions between the two particles become negligible.

Figure 2 shows two-proton correlation functions for energy gates containing different portions of equilibrium and nonequilibrium emission. Consistent with previous measurements [4,6–15], the correlation functions exhibit maxima at $q = 20$ MeV/c due to the attractive singlet S-wave final-state interaction. For low-energy protons ($E_p = 12$–16 MeV at $\Theta_A = 42°$ and $E_p = 12$–25 MeV at $\Theta_A = 109°$) the maxima are strongly attenuated, qualitatively consistent with an evaporative emission mechanism as suggested by the inclusive spectra. The maxima increase with the kinetic energy of the emitted particles, reaching values for $E_p = 50$–80 MeV which are the largest so far observed in medium-energy experiments [4,6–14], indicating rapid emission by a small source.

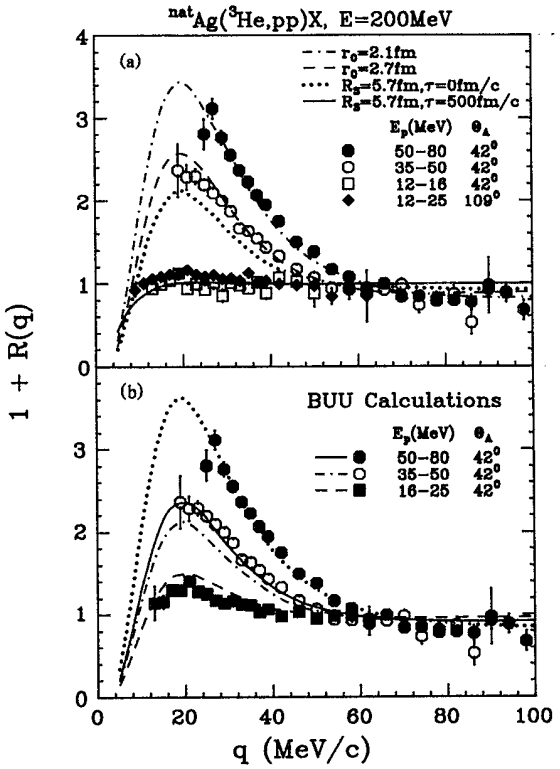

FIG. 2. (a) p-p correlation functions measured for the ^{3}He+Ag reactions at 200 MeV. The energy gates and angular locations of the center of the hodoscope are indicated in the figure. The curves are discussed in the text. (b) Comparison of experimental p-p correlation functions with predictions of the BUU theory for the ^{3}He+Ag reaction at 200 MeV. The dotted curve is discussed in the text.

Two-proton correlation functions may be calculated via the equation [1,3,5]

$$1+R(\mathbf{P},\mathbf{q}) = \int d^3r\,|\phi(\mathbf{q},\mathbf{r})|^2 \left| \frac{\int d^3X f(\mathbf{P}/2,\mathbf{X}+\mathbf{r}/2,t_>) f(\mathbf{P}/2,\mathbf{X}-\mathbf{r}/2,t_>)}{|\int d^3X f(\mathbf{P}/2,\mathbf{X},t_>)|^2} \right| . \quad (2)$$

Here, $\mathbf{P} = \mathbf{p}_1 + \mathbf{p}_2$ is the total momentum of the proton pair, and $\phi(\mathbf{q},\mathbf{r})$ is the two-proton relative wave function. The Wigner function $f(\mathbf{p},\mathbf{x},t_>)$ describes the phase-space distribution of protons of momentum $\mathbf{p}$ and position $\mathbf{x}$ at some time, $t_>$, after the emission process. It can be obtained from the probability, $g(\mathbf{p},\mathbf{r},t)$, for emitting a proton of momentum $\mathbf{p}$ at location $\mathbf{r}$ and time t by

$$f(\mathbf{p},\mathbf{r},t_>) = \int_{-\infty}^{t_>} dt\, g[\mathbf{p},\mathbf{r}-\mathbf{p}(t_>-t)/m,t] . \quad (3)$$

For illustration, the solid and dotted curves in Fig. 2(a) show correlation functions calculated assuming surface emission from an Ag targetlike residue ($R_S = 5.7$ fm), with an exponential time dependence given by

$$g(\mathbf{p},\mathbf{r},t) \propto \rho_0 \frac{d^3\sigma}{dp^3}(\hat{\mathbf{r}}\cdot\hat{\mathbf{p}})\Theta(\hat{\mathbf{r}}\cdot\hat{\mathbf{p}})\delta(R_S - r)\left[\frac{e^{-t/\tau}}{\tau}\right]\Theta(t) . \quad (4)$$

Here, ρ_0 is a normalization constant, $\Theta(t)$ is the unit step function, τ is the source lifetime, δ is the Dirac delta function, $\hat{\mathbf{r}}$ and $\hat{\mathbf{p}}$ are the unit vectors for position and momentum, and $d^3\sigma/dp^3$ is extrapolated from moving source fits to the single-proton inclusive spectrum, shown as the dashed lines in Fig. 1. The correlation functions for low-energy protons can be reproduced with lifetimes of $\tau \approx 300$–3000 fm/c; the solid curve shows a calculation for $\tau = 500$ fm/c. While larger maxima at $q = 20$ MeV/c are predicted for smaller τ, even the assumption of a vanishing source lifetime (dotted curve) underpredicts the correlation functions measured for the two highest-energy gates where nonequilibrium emission dominates. The dashed and dot-dashed curves show calculations for Gaussian sources of negligible lifetime,

$$g(\mathbf{p},\mathbf{r},t) \propto \rho_0 (e^{-r^2/r_0^2})\delta(t) , \quad (5)$$

with the specific source radii r_0 given in the figure. The calculations illustrate that the correlation functions for the most energetic protons are consistent with instantaneous emission by a system significantly smaller than the target nucleus.

Further insight can be obtained from the comparison, in Fig. 3, of the Gaussian source radii extracted from this experiment to radii extracted from measurements for ^{14}N, ^{16}O, and ^{40}Ar projectiles incident on heavy targets [6,9, 10,13]. To contrast the correlations of protons emitted at comparable stages of equilibration, these radii have been plotted as functions of v_p/v_{beam}, the ratio of v_p, the mean velocity of the detected protons, to v_{beam}, the velocity of the beam. For $v_p/v_{beam} \geq 0.7$, the extracted source radii for ^{14}N projectiles (open points and diamonds) decrease systematically with v_p/v_{beam}; the trend, interpolated by the solid line, is remarkably independent of the incident energy of the projectile. While the source radii for ^{16}O projectiles closely parallel those for ^{14}N projectiles, corresponding source radii extracted for ^{40}Ar (solid diamonds) and ^{3}He (solid points) projectiles are much larger and much smaller, respectively. The dot-dashed and dashed lines, in Fig. 3, are extrapolated from the solid line by multiplying the source radii for the solid line by the ratios $(40/14)^{1/3}$ and $(3/14)^{1/3}$, respectively. This agreement of extrapolated and measured source radii for ^{3}He and ^{40}Ar projectiles suggests that the spatial extent of the emitting region for energetic protons is governed initially by the overlap of these relatively small projectiles with the heavy target and, therefore, scales with the radius of the projectile. It is important to note that these simple trends, observed for $v_p/v_{beam} \geq 0.7$, would not be observed in energy averaged correlation functions, because such data primarily reflect the correlations of the more abundant low-energy protons where the correlation functions are more sensitive to emission time scales than to spatial source dimensions. Indeed for protons with $v_p/v_{beam} \lesssim 0.7$, the source radii for the three projectiles are comparable.

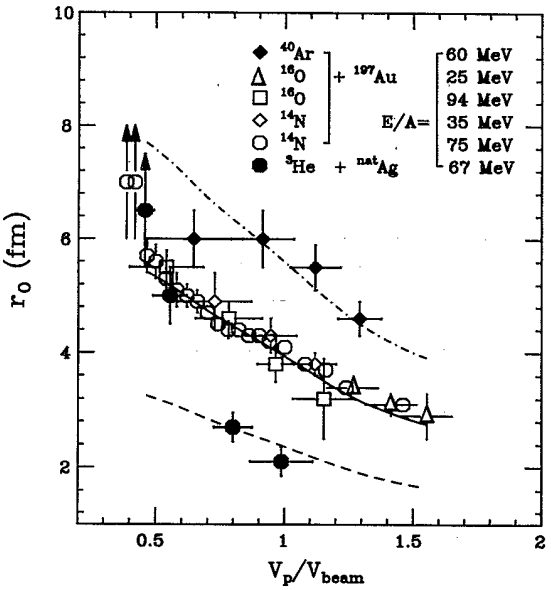

FIG. 3. Systematics of Gaussian source radii extracted for a variety of reactions. The solid and open points depict experimentally extracted source radii. The solid line is an interpolation of the source radii extracted for ^{14}N projectiles. The dashed and dot-dashed lines are extrapolated from the solid line via the ratio of the projectile radius to the radius of ^{14}N.

In order to determine whether the strong correlations observed in the present experiment can be reproduced by microscopic dynamical calculations, we have calculated correlation functions using Wigner transforms which satisfy the Boltzmann-Uehling-Uhlenbeck (BUU) transport equation [17,18]. This equation includes a self-consistent mean field, nucleon-nucleon collisions, and the Pauli exclusion principle, but does not describe the emission of clusters. In our calculations we assumed a free nucleon-nucleon cross section and an equation of state with a compressibility coefficient $K = 240$ MeV. Following Refs. [5] and [12], nucleon emission was calculated during a time interval of $\Delta t_e = 140$ fm/c after the initial contact of the colliding nuclei. Further details of the numerical procedure are given in Refs. [5], [12], and [19].

The nucleon differential cross sections at $\theta = 32.6°$ and 57.6° predicted by the BUU simulation are shown for $E \geq 30$ MeV by the solid histograms in Fig. 1 [20]. The dashed, dot-dashed, and solid curves in Fig. 2(b) show the correlation functions from the BUU calculations. For nonequilibrium emission at low ($E_p = 16$–25 MeV) and intermediate ($E_p = 35$–50 MeV) energies, the calculations are in reasonable agreement with the data. For the most energetic protons ($E_p = 50$–80 MeV), however, the calculations underpredict the observed correlations. For this energy gate the extracted source radius was smaller than the systematic extrapolation presented in Fig. 3, also suggesting an enhancement in the correlation function.

To explore whether this discrepancy may be a remnant of the spin correlation in the ^{3}He ground state, we varied

the relative weighting of the singlet and triplet states in the p-p relative wave function in Eq. (2) according to

$$|\phi(\mathbf{q},\mathbf{r})|^2=\alpha|\phi_s(\mathbf{q},\mathbf{r})|^2+(1-\alpha)|\phi_t(\mathbf{q},\mathbf{r})|^2, \quad (6)$$

where α is a weighting factor and $\phi_s(\mathbf{q},\mathbf{r})$ and $\phi_t(\mathbf{q},\mathbf{r})$ are the singlet and triplet spatial wave functions. Setting $\alpha=\frac{1}{4}$ selects the standard statistical weighting adopted for all calculations but those depicted by the dotted lines in Fig. 2(b). Choosing $\alpha=0.45$ raises the correlation function to values depicted by the dotted line in Fig. 2(b), comparable to the measured one. This value of α is consistent with the assumption that about 27% of the proton pairs in the highest-energy gate originated in the ^{3}He projectile and propagated to the detectors with their initial spin correlations undisturbed.

In summary, two-proton correlation functions measured for ^{3}He induced reactions on Ag at $E=200$ MeV increase dramatically with the energy of the detected protons. Combined with other correlation function data, these measurements suggest that the spatial extent of the emitting region is governed initially by the overlap of the projectile with the target. For proton energies with $E=16$–50 MeV, the measured trends are consistent with those predicted by the Boltzmann-Uehling-Uhlenbeck equation, suggesting that the localization in space-time of the emission of protons with these energies is reasonably well described by the model. The correlation functions of more energetic protons are underpredicted by the model, an effect which may reflect remnant spin correlations from the ground state of the ^{3}He projectile.

This work is based upon work supported by the National Science Foundation under Grants No. PHY-86-11210, No. PHY-89-13813, and No. PHY-89-06116, by the Department of Energy under Grant No. DE.FG02-88ER.40404.A000, and by a U.S. Presidential Young Investigator Award.

[1] S. E. Koonin, Phys. Lett. **70B**, 43 (1977).
[2] D. H. Boal and J. C. Shillcock, Phys. Rev. C **33**, 549 (1986).
[3] S. Pratt and M. B. Tsang, Phys. Rev. C **36**, 2390 (1987).
[4] D. H. Boal, C. K. Gelbke, and B. K. Jennings, Rev. Mod. Phys. **62**, 553 (1990).
[5] W. G. Gong, C. K. Gelbke, W. Bauer, N. Carlin, R. T. de Souza, Y. D. Kim, W. G. Lynch, T. Murakami, G. Poggi, D. P. Sanderson, M. B. Tsang, and H. M. Xu, Phys. Rev. C **43**, 781 (1991).
[6] W. G. Lynch, C. B. Chitwood, M. B. Tsang, D. J. Fields, D. R. Klesch, C. K. Gelbke, G. R. Young, T. C. Awes, R. L. Ferguson, F. E. Obenshain, F. Plasil, and R. L. Robinson, Phys. Rev. Lett. **51**, 1850 (1983).
[7] C. B. Chitwood, C. K. Gelbke, J. Pochodzalla, Z. Chen, D. J. Fields, W. G. Lynch, R. Morse, M. B. Tsang, D. J. Boal, and J. C. Shillcock, Phys. Lett. B **172**, 27 (1986).
[8] J. Pochodzalla, C. B. Chitwood, D.J. Fields, C. K. Gelbke, W. G. Lynch, M. B. Tsang, D. H. Boal, and J. C. Shillcock, Phys. Lett. B **174**, 36 (1986).
[9] J. Pochodzalla, C. K. Gelbke, W. G. Lynch, M. Maier, D. Ardouin, H. Delagrange, H. Doubre, C. Grégoire, A. Kyanowski, W. Mittig, A. Péghaire, J. Péter, F. Saint-Laurent, B. Zwieglinski, G. Bizard, F. Lefèbvres, B. Tamain, J. Québert, J. P. Viyogi, W. A. Friedman, and D. H. Boal, Phys. Rev. C **35**, 1695 (1987).
[10] Z. Chen, C. K. Gelbke, W. G. Gong, Y. D. Kim, W. G. Lynch, M. R. Maier, J. Pochodzalla, M. B. Tsang, F. Saint-Laurent, D. Ardouin, H. Delagragne, H. Doubre, J. Kasagi, A. Kyanowski, A. Péghaire, J. Péter, E. Rosato, G. Bizard, F. Lefèbvres, B. Tamain, J. Québert, and Y. P. Viyogi, Phys. Rev. C **36**, 2297 (1987).
[11] T. C. Awes, R. L. Ferguson, F. E. Obenshain, F. Plasil, G. R. Young, S. Pratt, Z. Chen, C. K. Gelbke, W. G. Lynch, J. Pochodzalla, and H. M. Xu, Phys. Rev. Lett. **61**, 2665 (1988).
[12] W. G. Gong, W. Bauer, C. K. Gelbke, N. Carlin, R. T. de Souza, Y. D. Kim, W. G. Lynch, T. Murakami, G. Poggi, D. P. Sanderson, M. B. Tsang, H. M. Xu, S. Pratt, D. E. Fields, K. Kwiatkowski, R. Planeta, V. E. Viola, and S. J. Yennello, Phys. Rev. Lett. **65**, 2114 (1990).
[13] W. G. Gong, C. K. Gelbke, W. Bauer, N. Carlin, R. T. de Souza, Y. D. Kim, W. G. Lynch, T. Murakami, G. Poggi, D. P. Sanderson, M. B. Tsang, and H. M. Xu, Phys. Rev. C **43**, 1804 (1991).
[14] D. A. Cebra, W. Benenson, Y. Chen, E. Kashy, A. Pradhan, A. Vandermolen, G. D. Westfall, W. K. Wilson, D. J. Morrissey, R. S. Tickle, R. Kortelling, and R. L. Helmer, Phys. Lett. B **227**, 336 (1989).
[15] G. N. Agakishiyev, R. R. Mekhteev, V. Boldea, S. Ditza, J. Bartke, M. Kowalski, D. Armutliyski, J. Bogdanowicz, A. P. Cheplakov, L. A. Didenko, A. P. Gasparian, V. G. Grishin, I. A. Ivanovskaya, T. Kanarek, E. N. Kladnitskaya, D. K. Kopylova, V. B. Lyubimov, K. Miller, V. F. Nikitina, J. Pluta, M. I. Soloviev, R. Togoo, G. P. Toneeva, M. Chubarian, R. N. Bekmirzayev, U. D. Sherkulov, Z. V. Metreveli, and Z. Strugalski, Z. Phys. A **327**, 443 (1987).
[16] T. Murakami, T. K. Nayak, W. G. Lynch, K. Swartz, Z. Chen, D. J. Fields, C. K. Gelbke, Y. D. Kim, M. R. Maier, J. Pochodzalla, M. B. Tsang, H. M. Xu, and F. Zhu, Nucl. Instrum. Methods Phys. Res. Sect. A **275**, 112 (1989).
[17] G. F. Bertsch, H. Kruse, and S. Das Gupta, Phys. Rev. C **29**, 673 (1984).
[18] G. F. Bertsch and S. Das Gupta, Phys. Rep. **160**, 189 (1988).
[19] W. Bauer, Michigan State University Report No. MSUCL-699 (unpublished).
[20] These nucleon spectra have been renormalized by the factor 0.4 to take into account the loss of flux due to the emission of neutrons and heavier composite light particles. Since this flux loss may be energy dependent this comparison is only qualitative.